Title
HIGH-RESOLUTION BETA- AMD GAMMA-RAY SPECTROMETER

Authors
Elad, Emanuel
Nakamura, MichiyukL.

Publication Date
1966-09-27

UCRL-17149

University of California

Ernest O. Lawrence Radiation Laboratory

HIGH-RESOLUTION BETA AND GAMMA-RAY SPECTROMETER

DISCLAIMER

For the 13th Nuclear Science Symposium,
IEEE, October 19-21, 1966, Boston, Mass.

UCRL-17149
Preprint

UNIVERSITY OF CALIFORNIA

Lawrence Radiation Laboratory
Berkeley, California

AEC Contract No. W-7405-eng-48

HIGH-RESOLUTION BETA- AND GAMMA-RAY SPECTROMETER

Emanuel Elad and Michiyuki Nakamura

September 27, 1966

HIGH-RESOLUTION BETA- AND GAMMA-RAY SPECTROMETER*

Emanuel Elad and Michiyuki Nakamura

Lawrence Radiation Laboratory
University of California
Berkeley, California

Summary

A high-resolution semiconductor beta- and gamma-ray spectrometer is described. The spectrometer consists of a silicon or germanium detector, low-noise field-effect transistor preamplifier, and a linear amplifier. The requirements for the different sections for high-resolution performance are outlined.

The detectors used are low-capacitance, low-leakage devices cooled to low temperatures. The preamplifier utilizes the low-noise characteristics of a cooled junction-field-effect transistor. These characteristics are described and several types of FET's are compared. A single FET, incorporated in a voltage-sensitive input stage, provides an optimum signal-to-noise ratio.

Pulse generator resolution of the preamplifier for zero external capacitance is 0.4 keV FWHM (Ge) with a slope of 0.038 keV/pF. Typical resolution obtained in the spectrometer in the low-energy region is 0.7 keV.

Recent measurements show that the cooling system is one of the main noise sources of the spectrometer. More than 20% improvement in resolution was observed in preliminary experiments when this noise source was suppressed.

Introduction

The development of semiconductor radiation detectors opened a new era to nuclear spectroscopy. The excellent resolution of these detectors, stemming from the small amount of energy needed to produce one electron-hole pair, improves the measurement precision of beta- and gamma-ray energies and enhances the ability to detect low-intensity peaks superimposed on a Compton continuum. However, the low level of the output signals necessitates low-noise preamplification to preserve the high resolving capabilities of the detector. Therefore, the resolution of a semiconductor spectrometer is determined by the detector-preamplifier section.

A large variety of germanium and silicon detectors has been developed in various laboratories[1-6] and their adaptability for high-resolution spectroscopy will be discussed here. The preamplifiers used with these detectors are distinguished by the active element used in the input amplifying stage. Following technological progress came the use of vacuum tubes,[7-9] bipolar transistors,[10-11] tunnel diodes[12] and field-effect transistors.[13-15] Most designs are based on charge-sensitive configurations, in an attempt to minimize the influence of long-term changes in detector capacitance.

This paper describes a high-resolution electron and gamma-ray spectrometer which was reported briefly elsewhere.[16-18] Low-capacitance, low-leakage silicon and germanium detectors are employed. The preamplifier is a field-effect-transistor (FET) type, designed to achieve an optimum signal-to-noise ratio. A voltage-sensitive, high-gain input stage is used, and gain losses due to input stray capacitance are minimized. The noise is reduced by cooling the FET, dc coupling the detector to the input stage of the preamplifier, and electrostatically shielding the input stage.

Pulse generator resolution of the preamplifier is 0.4 keV FWHM (Ge) for zero external capacitance with a slope of 0.038 keV/pF. The line widths of x-ray spectra (5 to 25 keV) measured with small silicon detector were 0.7 keV. A thin electron source measured with the same type of detector showed a resolution of 1.5 keV FWHM on a 90-keV line. Higher energy x rays (50 keV) and gamma rays (122 keV) measured with a small-volume germanium detector showed line widths of 0.67 and 0.8 keV FWHM, respectively.

General Considerations

A block diagram of the spectrometer is given in Fig. 1. The semiconductor detector and FET input stage of the preamplifier are mounted in a cryogenic chamber. The rest of the preamplifier input loop and cable driver is located outside the detector chamber. The linear amplifier, containing the pulse-shaping networks and the multichannel pulse-height analyzer, are commercially available units.

The resolution of the spectrometer is determined mainly by the input part of the system contained in the cryogenic chamber. Therefore, the design effort was concentrated on optimization of this part of the system. Let us thus now consider the elements of the input section, their specifications for a high-resolution system, and the configurational and environmental requirements.

Detector

The noise contributions of a semiconductor detector may be divided into:

1. Statistics of electron-hole production
2. Variations in charge collection times
3. Fluctuations in bulk and surface-leakage currents.

The effects of electron-hole-production statistics are summarized under Noise Considerations.

The variations in charge collection times cause a spread of the output pulse rise times. A wide-band amplifier may prevent the potential pulse-height fluctuations resulting from that spread, but on the other hand, a wider band of noise will be amplified. The spread in rise times will decrease with larger electrostatic fields generated by higher bias voltages applied to the detector. The limit here is the increasing leakage current of the back-biased diode.

The fluctuations in bulk-leakage currents are diminished by cooling of the detectors. Germanium detectors are operated at liquid nitrogen temperature, although no clear evidence is available that this is the optimum operating temperature. It was found[17] that silicon detectors give optimum noise performance at temperatures ranging from 120 to 140°K. The noise arising from surface-leakage current can be controlled by a guard-ring configuration.[19]

The output signal of a semiconductor detector is inversely proportional to the capacitance of the detector. Therefore, planar detectors with small area and large depletion depth are preferred for high-resolution spectroscopy. The low efficiency of such detectors is overcome by special fabrication methods[3, 20] giving high-volume, low-capacitance detectors.

To conclude, high-resolution spectroscopy requires low-leakage, low-capacitance detectors. In the described spectrometer, two types of lithium-drifted germanium detectors[1, 2] and one type of silicon detector[6] were used. The best resolution was obtained with 1 by 1 by 1 cm Berkeley type[1] and 3 by 1.5 by 0.3 cm Livermore type[2] germanium detectors and with 5-mm-diameter, 3-mm-thick silicon detectors. The leakage current of all these detectors, at the appropriate bias voltages, was less than 10^{-10} A.

Input Stage of the Preamplifier

Active Device. The inherent low noise of the field-effect transistor made it an attractive candidate for the active input device of high-resolution preamplifiers. The signal-to-noise ratio of an FET increases significantly at low temperatures. It is relatively easy and natural to take advantage of this feature when the FET is operated in conjunction with cooled semiconductor detectors. Figure 2 shows a typical dependence of FET's forward transconductance (g_m) on temperature with pinch-off voltage as a parameter. The optimum point, a function of the pinch-off voltage, appears at lower temperature for devices having higher pinch-off voltages. This optimum point varies from one type of FET to another. For n-channel silicon devices having 2.5 volts pinch-off voltage, the measured optimum g_m points are summarized in Table I. The optimum temperature region of the 2N3823 is -160 to -180°C for devices with pinch-off voltages ranging from 2 to 5 volts.

The noise characteristics of an FET, described briefly in the next section, vary widely and

Table I. FET optimum temperature for maximum g_m.

Manufacturer	FET type	Temp for max g_m (°C)
Texas Instruments	2N3823	-165
Motorola	2N4221	-180
Motorola	2N4223	-190
Union Carbide	UC210	-196
Union Carbide	UC240	-155
Union Carbide	2N4416	-170

appear unpredictable from the electrical parameters. Figure 3 shows the noise versus temperature characteristics of an FET measured with a wideband rms voltmeter. No correlation between the noise and pinch-off voltage is evident. Most of the low-noise units of the 2N3823's have their minimum noise in the temperature range of -140 to -175°C. Although some of the units exhibit large noise fluctuations, the noise characteristic in its minimum range is sufficiently flat to allow noncritical engineering solutions.

We chose the Texas Instrument Company's 2N3823 for our preamplifier, because it was the best FET available at the time this preamplifier was designed. Now newer devices such as Motorola's 2N4221 or Union Carbide's 2N4416 give comparable performance at lower cost. From our measurements on the 2N3823 (Figs. 2 and 3) we concluded that the optimum temperature range for low-noise amplification with that device is -150 to -180°C.

The mechanical set-up used in the spectrometer to cool the FET to liquid nitrogen temperatures is described under Detector and FET mountings. Due to several inherent thermal resistances, the case temperature of the FET, dissipating around 100 mW, ranged from -160 to -170°C. Therefore, to keep the system simple, no external means were provided to vary the temperature of the FET. Results improved by 5 to 10% may be expected if each unit were adjusted to its optimum temperature.

Input-Stage Configuration. A very popular[8, 9, 13, 14] input-stage configuration used in low-noise amplifiers is the cascode connection. Commonly used in VHF and UHF amplifiers, it practically eliminates the Miller capacitance. However, in most cases the time response of semiconductor detectors does not require the use of VHF techniques. Cascode connection was used by the designers of vacuum tube amplifiers to overcome the lower gain of a triode and the higher noise of a pentode. The availability of a high-gain, low-noise common source FET stage eliminates the necessity of a cascode connection. Theoretically, therefore, with a high-gain input stage, the difference between cascode and cascade configurations should be negligible. In practice we found that a cooled FET input stage

with a cascode connection is the nosier one.

Two commonly used preamplifier configurations are the charge-sensitive and voltage-sensitive circuits. The main advantage of the charge-sensitive configuration is the independence of output pulse height on detector capacitance. In contrast, the voltage-sensitive circuit has a higher signal-to-noise ratio and therefore is preferred for a high-resolution system. Lithium drifted detectors and, particularly, totally depleted detectors have relatively constant capacitance, which offsets the disadvantage of the voltage-sensitive circuit.

Figure 4 shows the input stage of the decribed preamplifier. A voltage-sensitive, common-source stage is used. The FET is dc coupled to the detector, with the detector's resistance serving as the gate resistor. This configuration eliminates the stray capacitance of the coupling capacitor and of the biasing resistors for the detector and the FET. The eliminated noise sources are: leakage current of the coupling capacitor, thermal noise of the biasing resistors, and thermoelectric voltages generated by the additional soldering points on the input lead. The bias of the FET is determined by the leakage resistances of the detector and the FET; it may be adjusted by varying the voltage V_1 and is temperature stable because both the FET and the detector are held at constant temperature.

The input stage shown in Fig. 4 exhibits very low noise, and is therefore suitable for a high-resolution system. When high resolution is not the primary objective of the system, the charge-sensitive configuration shown in Fig. 5 is used; it is intended for higher capacitance or higher leakage detectors and is slightly less affected by high count rates.

Noise Considerations

Detector

The noise components contributed by the detector were outlined in the preceding section. Here we discuss briefly the statistics of electron-hole formation. With the assumption of Gaussian distribution, the statistical spread in pulse height, expressed in units of energy, is

$$W = 2.36\sqrt{FE\epsilon} \qquad (1)$$

where
- W = line width expressed in FWHM
- F = Fano factor
- E = energy in eV
- ϵ = average energy required to produce one electron-hole pair.

Equation (1) shows that statistical fluctuations limit the resolution obtainable for high energies.

In the described spectrometer the energy spread of 50 keV x rays due to statistics (F = 0.2; ϵ = 2.9 eV) equals the spread due to electronic noise. Therefore, due to quadratic addition of noise sources, any substantial improvement in resolution for energies greater than 200 keV will come with better detector materials having smaller Fano factors[21] or smaller ϵ's.

Field-Effect Transistor

The basic noise source in FET's is the thermal noise of the conducting channel.[22] The other noise sources such as leakage current or gate noise current caused by noise modulation of the depletion layer width are comparatively negligible.

The thermal noise can be expressed as equivalent noise resistance

$$R_n = \frac{0.7}{g_m} \qquad (2)$$

or as an equivalent noise charge[1] (ENC) expressed in electron-hole pairs

$$(ENC)^2 = bC_t^2 R_n T \qquad (3)$$

where
- b = a constant
- C_t = input capacitance
- g_m = transconductance
- T = absolute temperature

and

$$C_t = C_{gs} + C_D + C_s \qquad (4)$$

- C_{gs} = gate to source capacitance of the FET
- C_D = detector capacitance
- C_s = stray and feedback capacitance.

Combining equations (2), (3), (4) we get

$$(ENC)^2 = b_1 \frac{T(C_{gs}+C_D+C_s)^2}{g_m} . \qquad (5)$$

For n-paralleled FET's

$$(ENC)^2 = b_1 \frac{T(nC_{gs}+C_D+C_s)^2}{n \cdot g_m} . \qquad (6)$$

Optimal signal-to-noise ratio requires a minimum ENC, as the signal charge is constant for a given energy. From Eq. (6) we get

$$\frac{d(ENC)}{dn} = 0 . \qquad (7)$$

The optimum number of paralleled FET's from Eqs. (6) and (7) is

$$n = \frac{C_D + C_s}{C_{gs}} . \qquad (8)$$

For high-resolution spectroscopy in which low capacitance detectors are used

$$C_{gs} \approx C_D + C_s . \qquad (9)$$

Therefore, it is clear from Eq. (8) that paralleling FET's is disadvantageous for high-resolution systems. From Eq. (5) we see also that the noise of a cooled FET preamplifier should decrease as T^k ($0.8 < k < 1.5$), taking into account the change of g_m with temperature (see Fig. 2). This kind of behavior was observed in general (see Fig. 3) only for some of the FET's. The observed noise fluctuations are not explained by the basic mechanism of the FET and probably are a function of the fabrication process.

Preamplifier Circuit

The complete schematic of the preamplifier is given in Fig. 6. The circuit can be divided into two parts, the input section and the cable driver. The voltage-sensitive input section (upper circuit) as well as the charge-sensitive configuration (lower circuit) are shown.

The input section consists of the common-source FET stage Q_1, emitter-follower Q_2, and the difference amplifier Q_3 and Q_4. The FET is mounted in the detector's cryogenic chamber (dashed line). The chamber provides very effective shielding against low-frequency noise, a condition that is essential for the high-gain input stage. The load of the input stage consists of the R_1, C_1 network. The low pass characteristics of the load ensure the attenuation of high-frequency components of the noise. The difference amplifier Q_3, Q_4 with series emitter resistors R_2, R_3 provides high-voltage gain that is insensitive to variations of transistor parameters. The dc balancing of the amplifier is done with potentiometer R_4. The two separate outputs of the difference amplifier offer more ideal feedback path for the charge-sensitive configuration than single ended amplifiers. The voltage gain of the input section is 200, and is increased to 1000 for the charge-sensitive configuration by changing R_2 and R_3 to 10 ohms. Low f_t transistors were used as Q_2 through Q_5 for high-frequency noise filtration.

The cable driver consists of emitter follower Q_5 and a feedback amplifier Q_6, Q_7. The voltage feedback used in the amplifier ensures the low output impedance of the preamplifier. The gain of the amplifier Q_6, Q_7 is determined by resistors R_5, R_6, and R_7.

The preamplifier can process input signals with either polarity and gives an inverted output pulse. The high-voltage bias is applied to the detector through the R_8, C_2 network. The 1-sec integrator prevents high-voltage transients at the gate of the FET when the detector bias is applied.

Detector and FET Mountings

The low temperatures at which germanium and silicon detectors operate require the use of vacuum-tight cryogenic chambers. The cold surface of the chamber, through which the detector is cooled, is generally at ground potential. Direct coupling between the detector and the input stage of the preamplifier requires insulation of the detector from ground. The constraint on the insulator is that it has to be a good heat conductor.

In the described spectrometer, sapphire and ceramic rods are used as insulators for germanium and silicon detectors, respectively. Figure 7 shows the front end of a germanium spectrometer. A thin Mylar strip attaches the detector to a metal plate through which the high voltage is applied. A small copper contact pressed by the Mylar strip provides the gate connection and minimizes the input stray capacitance. The FET is mounted on an aluminum stud fixed on the cold surface, and is held in a TO-18 heat sink (type TX 1808-7, IER Corp).

The silicon spectrometer mounting, similar to that discussed above, was described previously.[17] The optimum temperature for the silicon detector was determined by the size of the ceramic rods. The details of the mountings and the housing arrangements for the germanium and silicon detectors will be available in a separate report.[23]

Experimental Results

Preamplifier

Measurements were made to determine the yield of low-noise FET's from commercially available devices. The criterion for a low noise device was to assure a 1-keV resolution or better for the γ rays of ^{57}Co. The results obtained on 2N3823 (Texas Instruments) are shown in Fig. 8. The signal-to-noise ratio of 50 units was measured, 10 in each of the indicated ranges of the saturation current (I_{dss}). The overall yield for the 2N3823 is 35%. A similar yield figure was obtained on a smaller sample of 2N4221 (Motorola) transistors.

The preamplifier circuit was built on a regular printed circuit board. Lay-out of the components and the length of the connecting wires from the input stage were not critical. The preamplifier circuit is enclosed in a metal box, but careful shielding is not required. The input stage is of course well shielded by the metal cryogenic chamber.

The performance characteristics of the preamplifier are:

1. Passive input capacitance – 5 pF.
2. Maximum terminated output voltage – 5 V.
3. Integral linearity – better than 0.1%.
4. Noise referred to input – 0.3 μV rms or equivalent noise charge 60 electrons rms.
5. Output pulse rise time – 0.2 μsec.
6. Output pulse decay time – 200 μsec.
7. Voltage gain – 3000 or 1000.
8. Gain stability with change of the count rate by 10^4 pps – better than 0.2%.

A pulse generator test of the preamplifier was carried out with a RIDL mercury-relay-type pulse generator and a 0.5-pF test capacitor. Pulse-generator resolution of the voltage-sensitive configuration was 0.4 keV (Ge) FWHM with

zero external capacitance. The resolution of the charge-sensitive circuit is 0.65 keV (Ge) FWHM. The resolution versus input capacitance for the two configurations is shown in Fig. 9. For low external capacitance, 0 to 3 pF, the rate at which the resolution deteriorates is approximately 38 eV/pF for both configurations. For higher input capacitance (as much as 10 pF) the slope of the voltage-sensitive curve increases (80 eV/pF at 10 pF) while the slope of the charge-sensitive circuit remains almost constant. However, it can be seen from Fig. 9 that for detectors having less than 10 pF capacitance, the voltage-sensitive input stage is superior.

The influence of noise from the second stage on the resolution of the preamplifier was determined by using different amplifiers cascaded with the input stage. A vacuum-tube-type preamplifier and transistorized commercial units were used. In all cases the changes in resolution were negligible.

No long-term instabilities (6 months) due to the voltage-sensitive input stage were observed.

Spectrometer

Two types of germanium detectors were used in the γ-ray spectrometer: LRL-Livermore type[2] (3 by 1.5 by 0.3 cm) and LRL-Berkeley type[1] (1 by 1 by 1 cm). Both detectors have capacitances between 1 and 2 pF and 0.1 A leakage current. The bias voltages of the Livermore type range from 1000 to 2000 V, and for the Berkeley type from 600 to 1400 V. The detector is kept in vacuum of $2 \cdot 10^{-7}$ torr.

The signal obtained from the detector was processed by the described preamplifier with a voltage-sensitive input stage and by a Tranlamp[24] linear amplifier. Although several commercial amplifiers, such as the Tennelec TC200, were tried, they had negligible effect on the resolution. The signal was shaped with single differentiation and integration network having 5-μsec and 0.5-to-1 μsec time constants, respectively. System resolution was not critical with the pulse-shaping time constants. Different multi-channel pulse-height analyzers such as Nuclear Data and RIDL were used in the spectrometer.

The measured resolution of the spectrometer as a function of energy is shown in Fig. 10. The resolution for 50-keV x rays is 0.67 keV and for ^{57}Co γ rays is 0.8 keV. A typical x-ray spectrum of ^{68}Er is shown in Fig. 11. In this spectrum the $K_{\alpha 1}$ and $K_{\alpha 2}$ lines, which are only 0.9 keV apart, are clearly resolved. The dead layer of germanium detectors limits the range of the spectrometer to energies higher than 35 keV.

Spectroscopy of low-energy x rays and electrons was done with a silicon detector. LRL-Berkeley type,[6] 2-pF crystal was used (5-mm diameter, 3-mm thick). The bias voltage for this type of detector is in the range of 150 to 250 V. The silicon spectrometer had the same electronics as the germanium system.

The measured resolution of the silicon system as a function of energy is shown in Fig. 10. The resolution for 6.4-keV ^{57}Fe x rays is 0.7 keV, and for 13.96-keV ^{241}Am x rays is 0.75 keV. The x-ray spectrum of ^{241}Am is shown in Fig. 12.

The performance of the silicon spectrometer for electrons was tested with ^{237}U source. The obtained spectrum, electrons and γ-rays, is shown in Fig. 13. The resolution for electrons measured from the 89.4-keV energy line was 1.5-keV FWHM. The uranium source was a film layer less than 7 $\mu g/cm^2$ thick. A thin source is an essential requirement for high-resolution electron spectroscopy.

Electronic noise limits the range of the silicon spectrometer to energies greater than 2 keV.

Conclusions

A high-resolution beta- and gamma-ray spectrometer was described. It consists of a semiconductor silicon or germanium detector, a low-noise field-effect transistor preamplifier, and a linear amplifier.

Low-capacitance, low-leakage detectors, cooled to liquid nitrogen temperatures, are used. The preamplifier utilizes the low-noise characteristics of a cooled junction-field-effect transistor. A single FET incorporated in a voltage-sensitive input stage provides optimum signal-to-noise ratio. Mounting the FET in the cryogenic chamber and coupling it directly to the detector minimizes the parasitic noise sources. A very simple configuration of the input section, particularly suited for an integrated circuit arrangement, is thus achieved.

Pulse generator resolution of the preamplifier for zero external capacitance is 0.4-keV FWHM (Ge) with a slope of 0.038 keV/pF. Typical resolution obtained with the spectrometer in the low-energy region is 0.7 keV.

Recent investigation shows that one of the main noise sources present in the described spectrometer is the cooling system. The constant boiling of liquid nitrogen generates mechanical vibrations of the cold surface. The exact mechanism of transforming this mechanical noise into electrical signal is not yet completely understood. Although the resulting noise is mainly of low frequency (1 kHz), the interfering high-frequency components are relatively intense. Results of preliminary measurements made after suppression of the described noise are illustrated by the ^{241}Am spectrum in Fig. 14. The resolution was improved by more than 20%, as demonstrated by the separation of $K_{\beta 1}$ and $K_{\beta 2}$ lines only 0.81-keV apart. We believe that complete elimination of the noise generated by the cooling system will improve the resolution of the spectrometer beyond 0.5 keV.

Acknowledgments

Many people have contributed ideas and effort to this article. In particular we would like to thank John J. Griffin and Richard C. Jared for their technical assistance. Our thanks are also due to the experimenters in the Nuclear Chemistry Department of LRL for their cooperation and interest in the described topic.

Footnotes and References

*Work performed under the auspices of the U. S. Atomic Energy Commission.

1. F. S. Goulding, Lawrence Radiation Laboratory Report UCRL-16231, July 1965 (unpublished).
2. G. A. Armantrout and D. C. Camp, Lawrence Radiation Laboratory Report UCRL-12333, February 1965 (unpublished).
3. G. A. Armantrout, IEEE NS-13 No. 3 (1966), 328.
4. H. L. Malm, IEEE NS-13, No. 3 (1966), 285.
5. A. J. Tavendale, Nucl. Instr. Methods 36 (1965), 325.
6. R. P. Lothrop and H. E. Smith, UCRL-16190, June 1965 (unpublished).
7. E. Fairstein, NRC Publ. No. 871 (September 1960), 210.
8. R. L. Chase, W. A. Higinbotham, and G. L. Miller, IRE NS-8, No. 1 (1961), 147.
9. J. L. Blankenship, IEEE NS-11, No. 3 (1964), 373.
10. A. W. Pryor, Nucl. Instr. Methods 6 (1960), 164.
11. T. L. Emmer, IRE NS-9, No. 3 (1962), 305.
12. L. G. Jonasson, Nucl. Instr. Methods 26 (1964), 104.
13. V. Radeka, Brookhaven National Laboratory Report BNL-6953 (1963).
14. T. W. Nybakken and V. Vali, Nucl. Instr. Methods 32 (1965), 121.
15. K. F. Smith and J. E. Cline, IEEE NS-13, No. 3 (1966), 468.
16. E. Elad, Nucl. Instr. Methods 37 (1965), 327.
17. E. Elad and M. Nakamura, Nucl. Instr. Methods 41 (1966), 161.
18. E. Elad and M. Nakamura, Nucl. Instr. Methods 42 (1966), 315.
19. A. J. Tavendale, Nucl. Instr. Methods 36 (1965), 1275.
20. G. A. Armantrout, to be published in IEEE Transactions on Nuclear Science, 13th Nuclear Science Symposium, Boston, 1966.
21. H. M. Mann, H. R. Bilzer, and I. S. Sherman, IEEE NS-13, (1966), 252.
22. Van der Ziel, Proc. IRE 50 (1962), 1808.
23. C. Eugene Miner (Lawrence Radiation Laboratory), private communication.
24. W. Goldsworthy, Lawrence Radiation Laboratory circuit diagram 15X4845C.

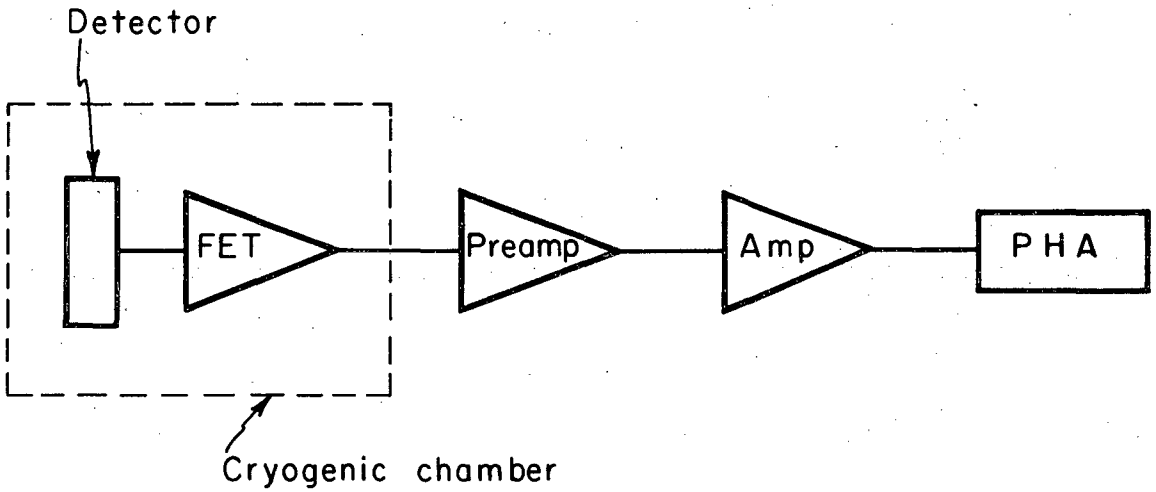

Fig. 1. Block diagram of the spectrometer.

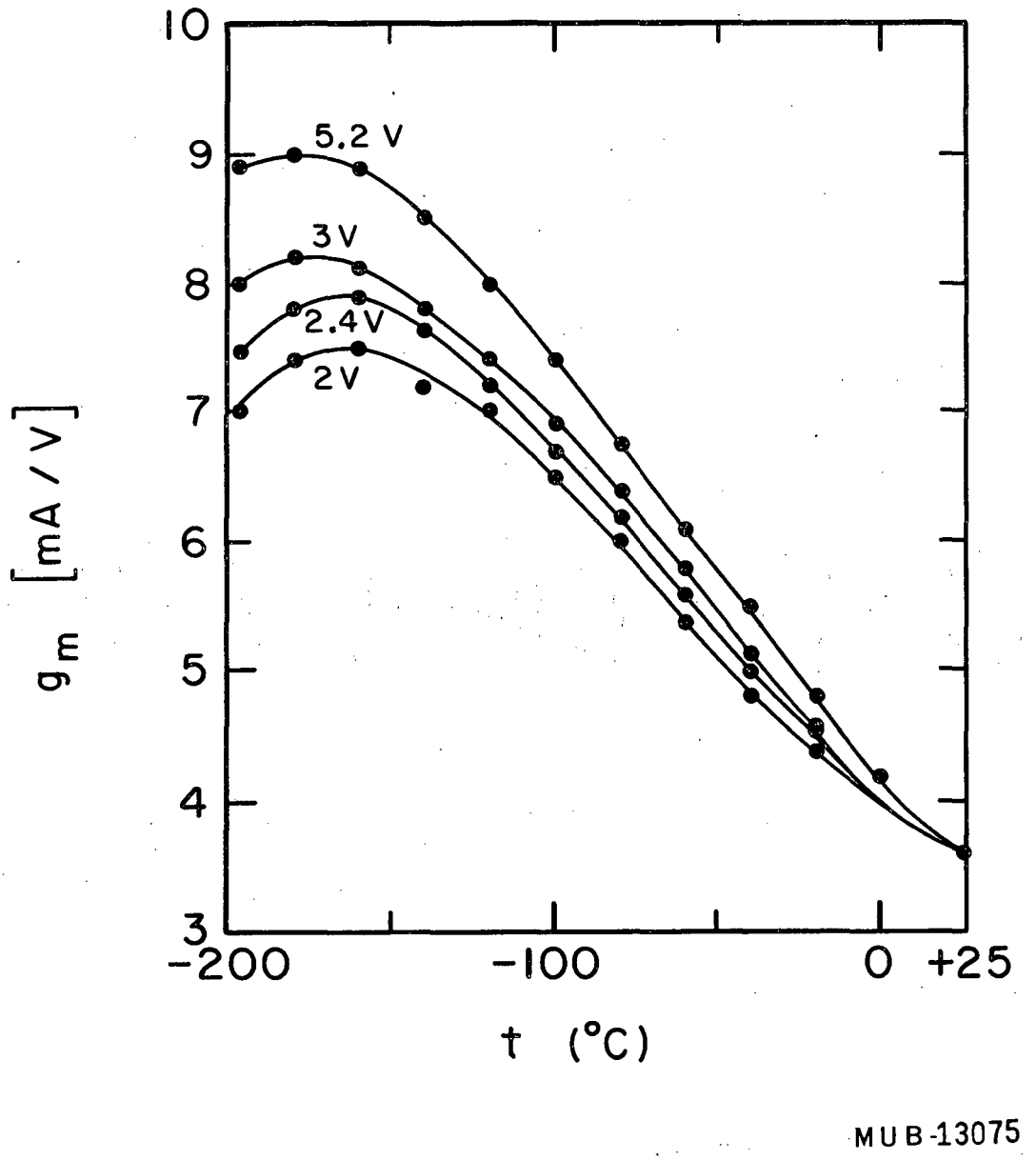

Fig. 2. Transconductance of 2N3823 versus temperature with pinch-off voltage as a parameter; tranconductance is normalized to 3600 μmhos at 25° C.

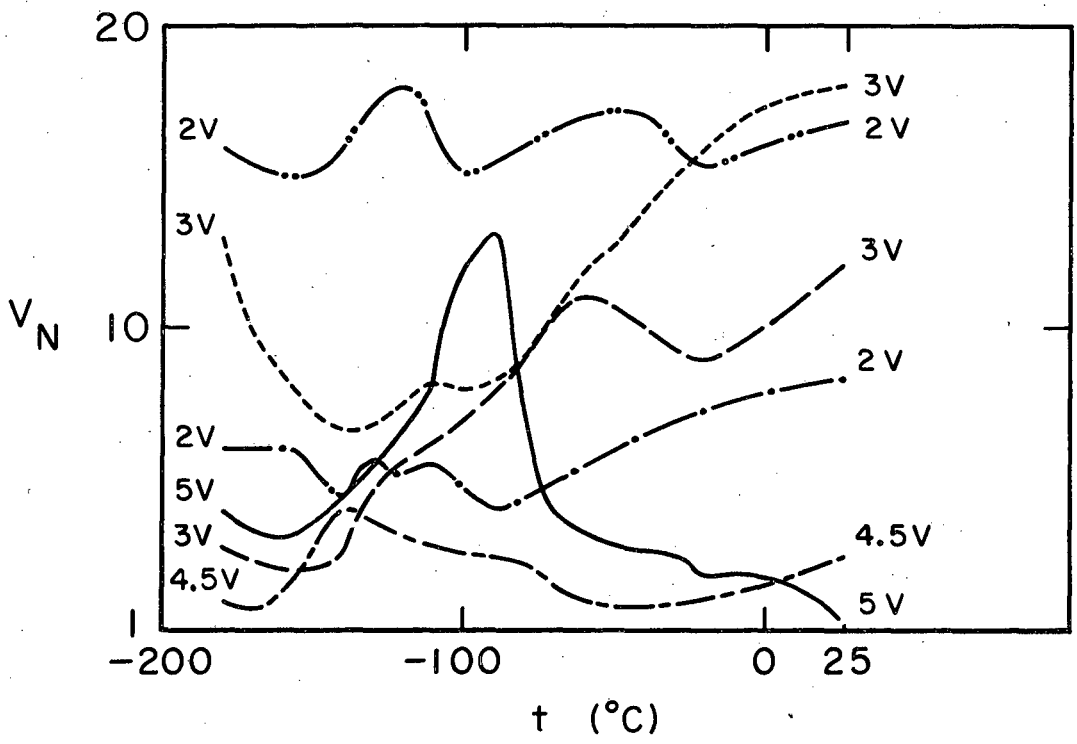

MUB-13076

Fig. 3. Noise of 2N3823 versus temperature.

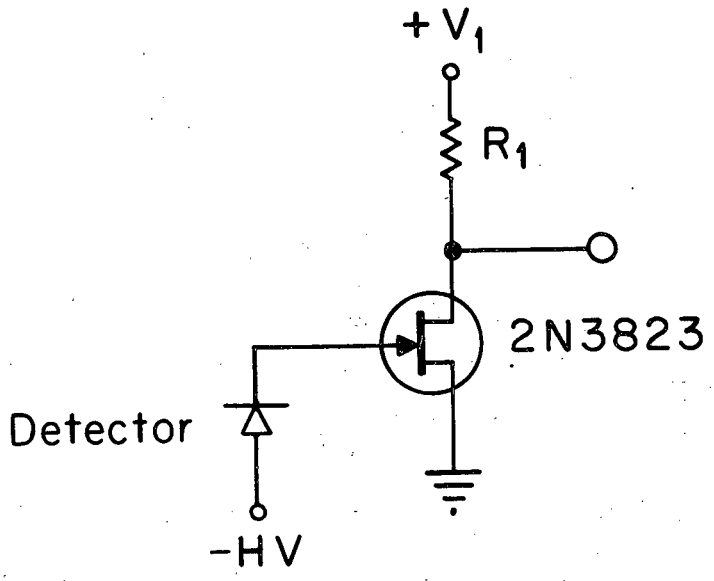

Fig. 4. Voltage-sensitive input stage.

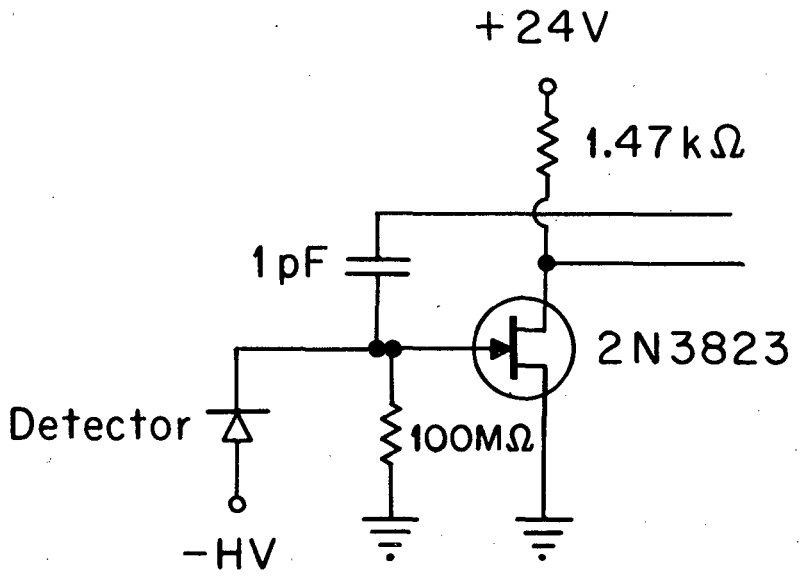

Fig. 5. Charge-sensitive input stage.

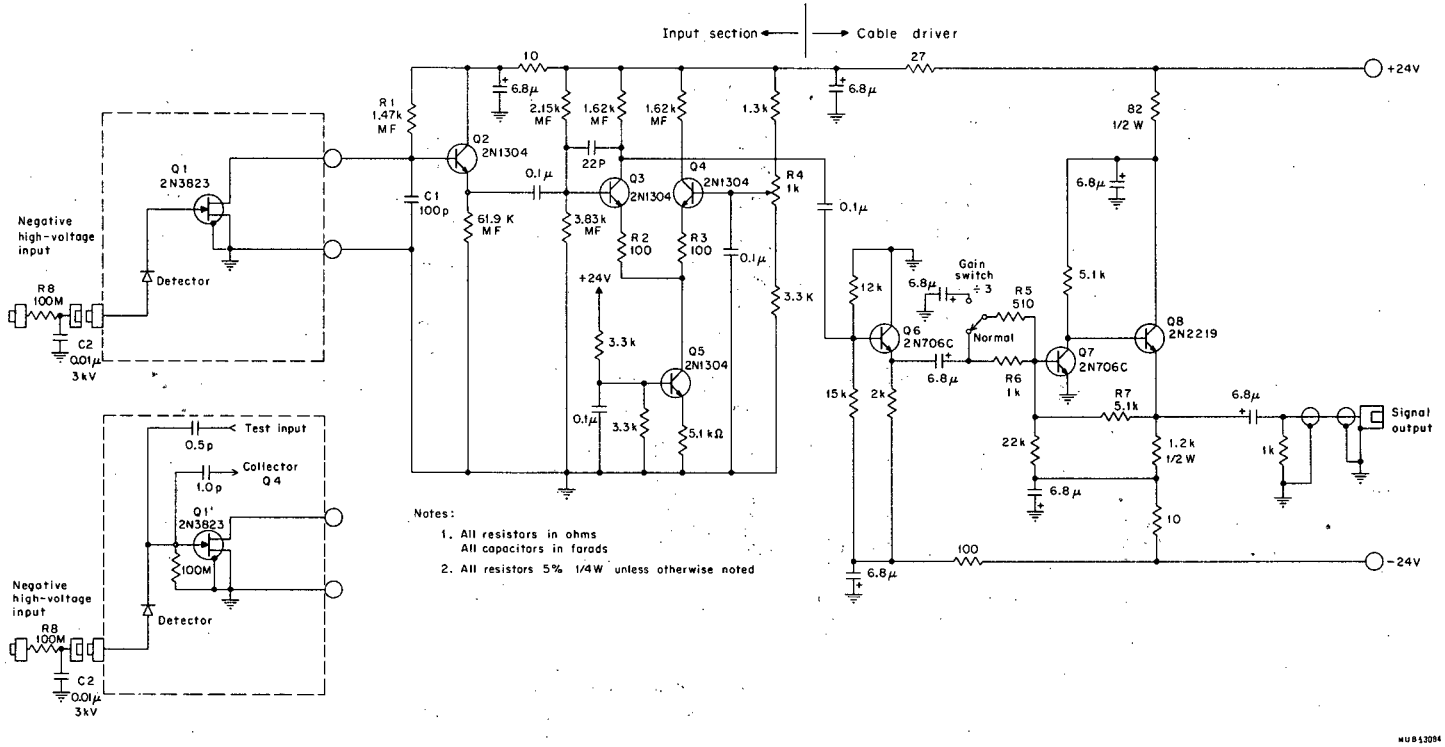

Fig. 6. Circuit diagram of the preamplifier.

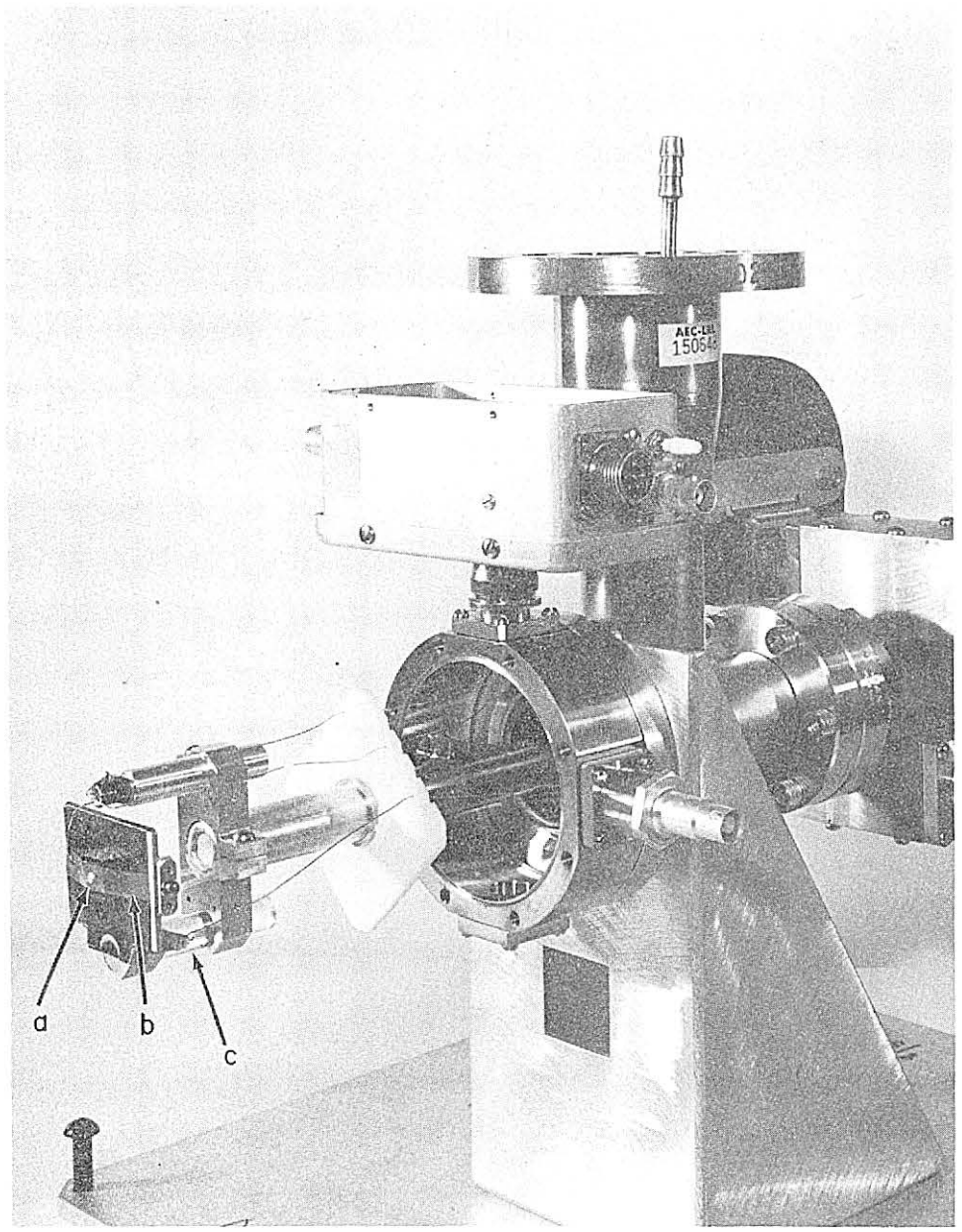

ZN-5947

Fig. 7. Front end of a germanium spectrometer.
a. Copper contact; b. Mylar strip; c. Sapphire rod.

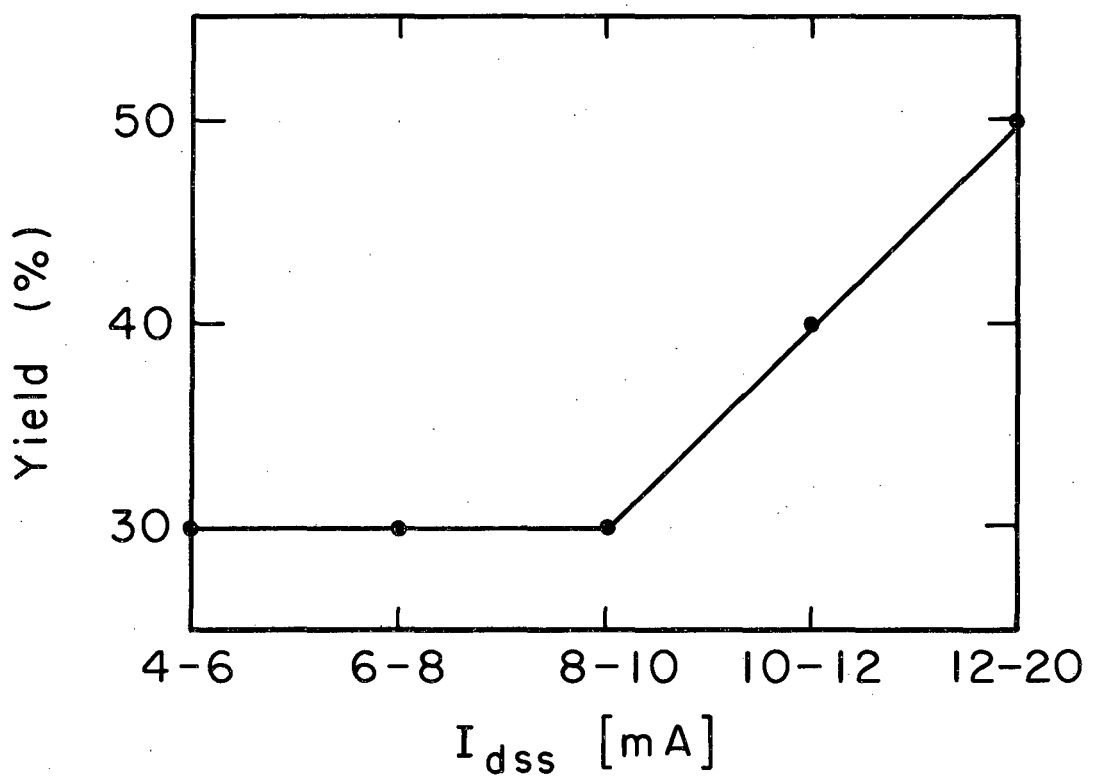

Fig. 8. Yield of low noise 2N3823 FET's (Texas Instrument Co.).

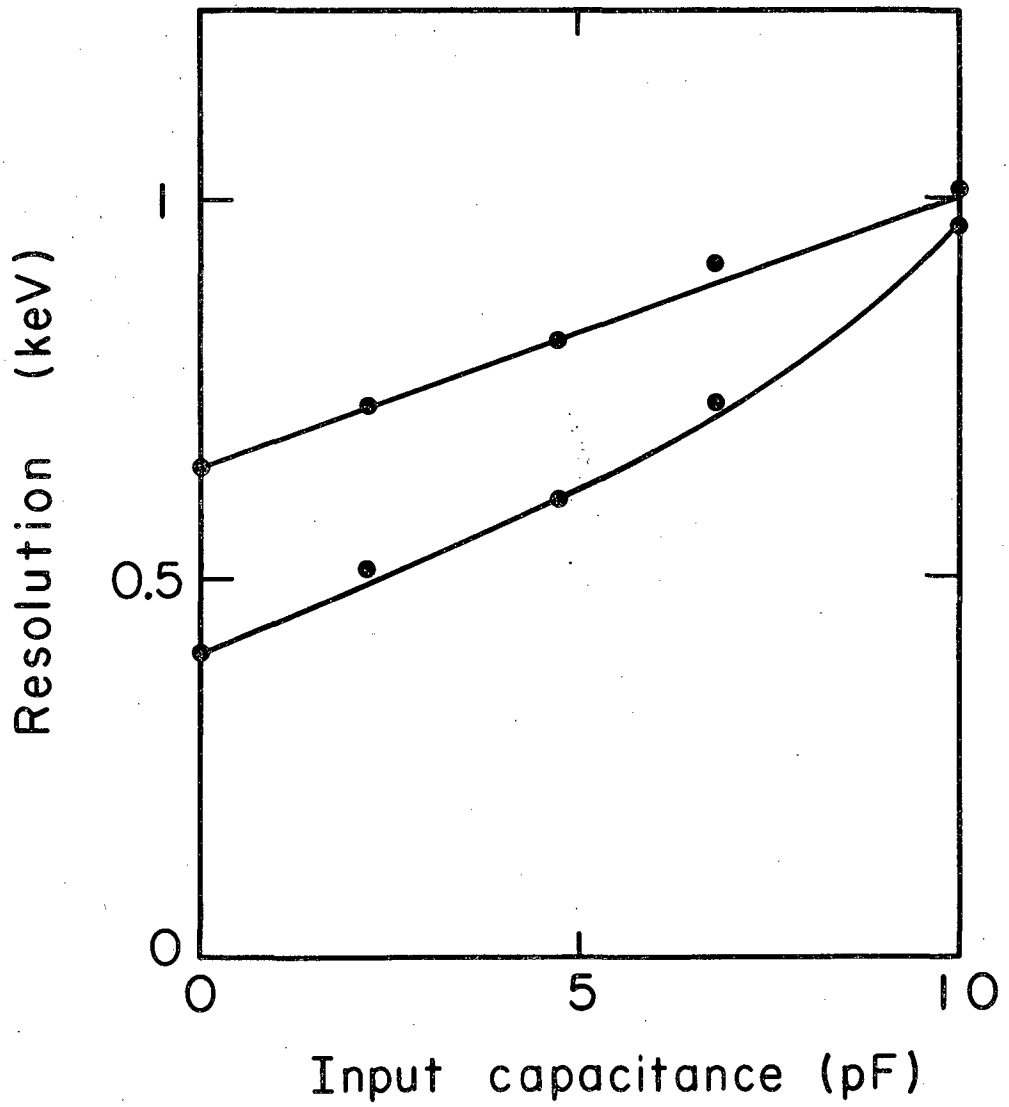

Fig. 9. Resolution versus input capacitance of the preamplifier.

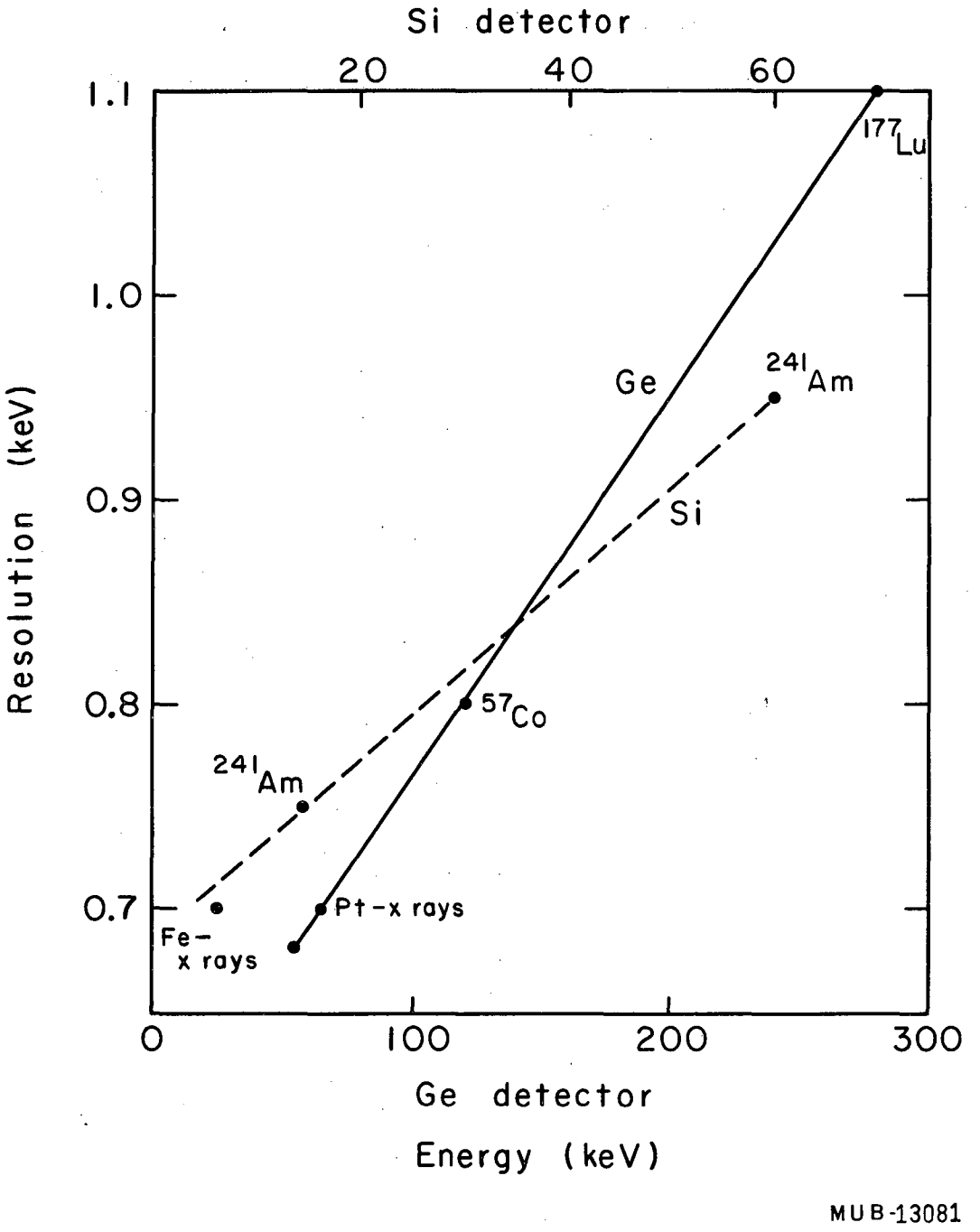

Fig. 10. Resolution versus energy.

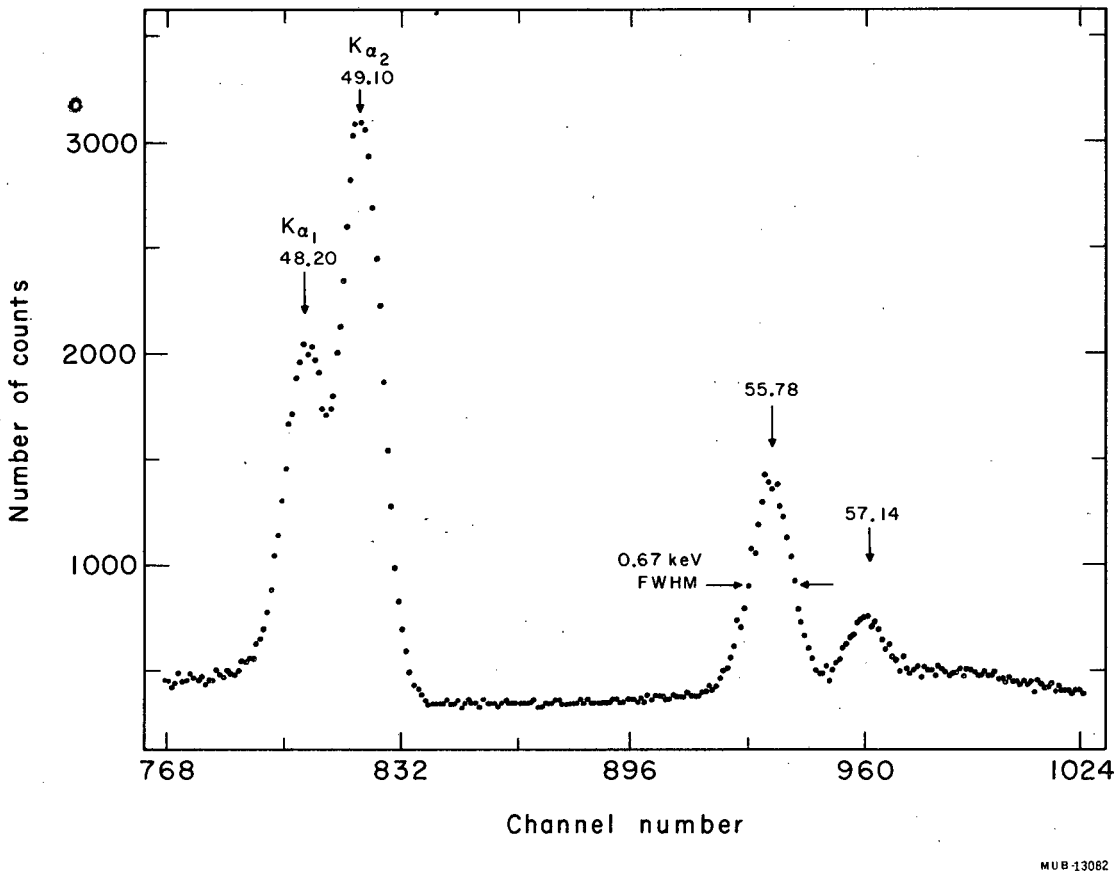

Fig. 11. X-ray spectrum of ^{68}Er. Energy in keV.

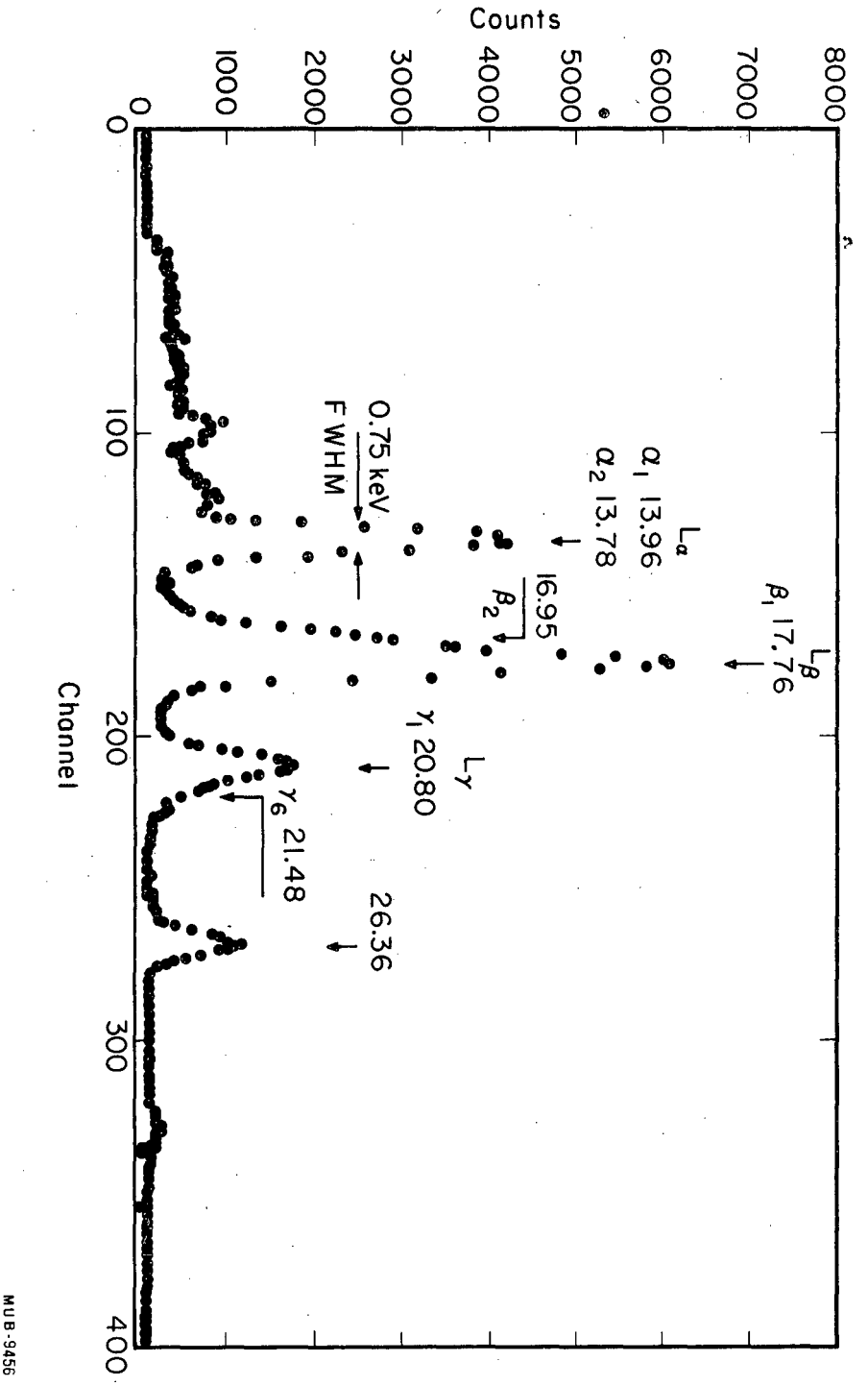

Fig. 12. X-ray spectrum of ^{241}Am. Energy in keV.

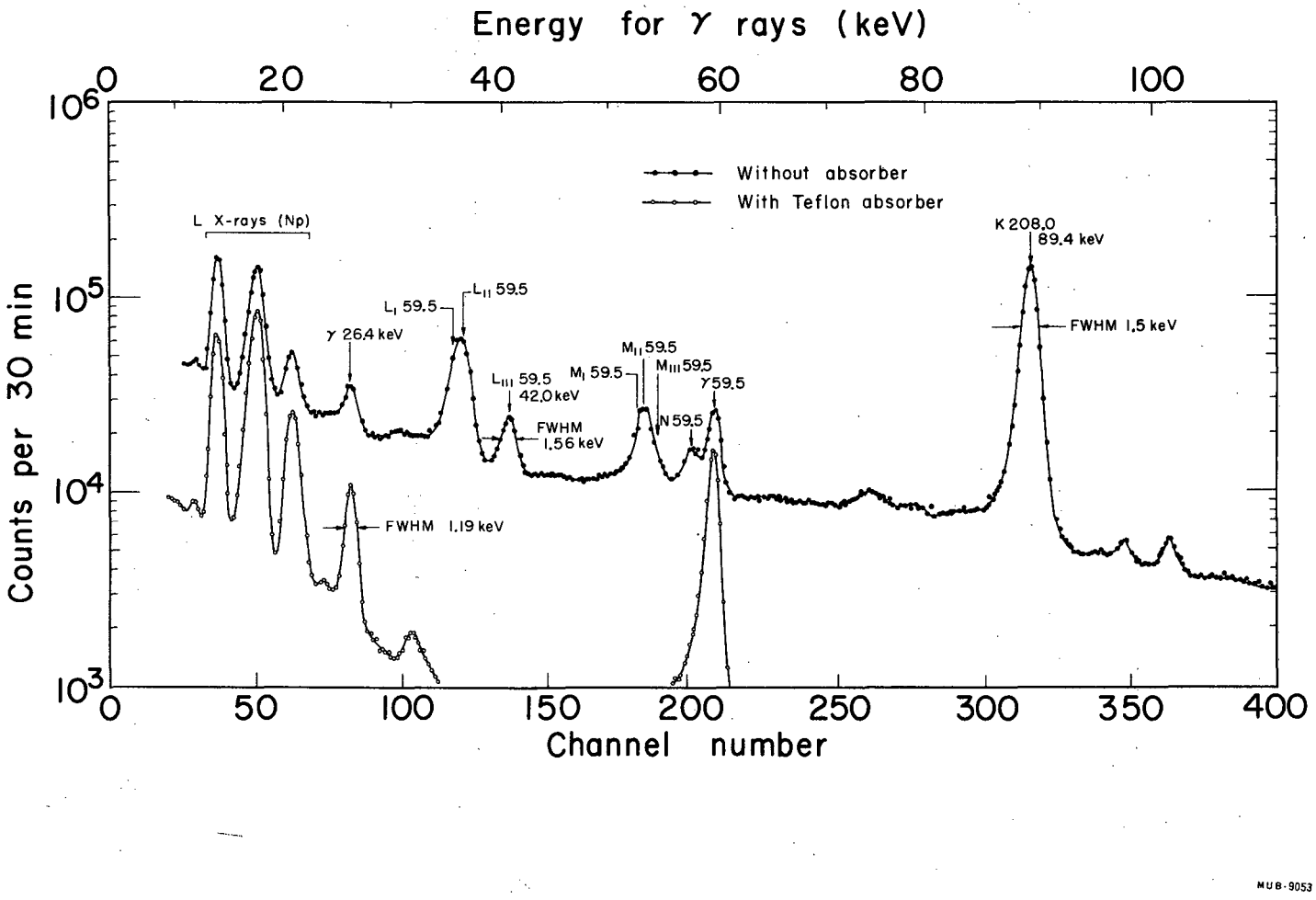

Fig. 13. Electron and γ-ray spectra of ^{237}U.

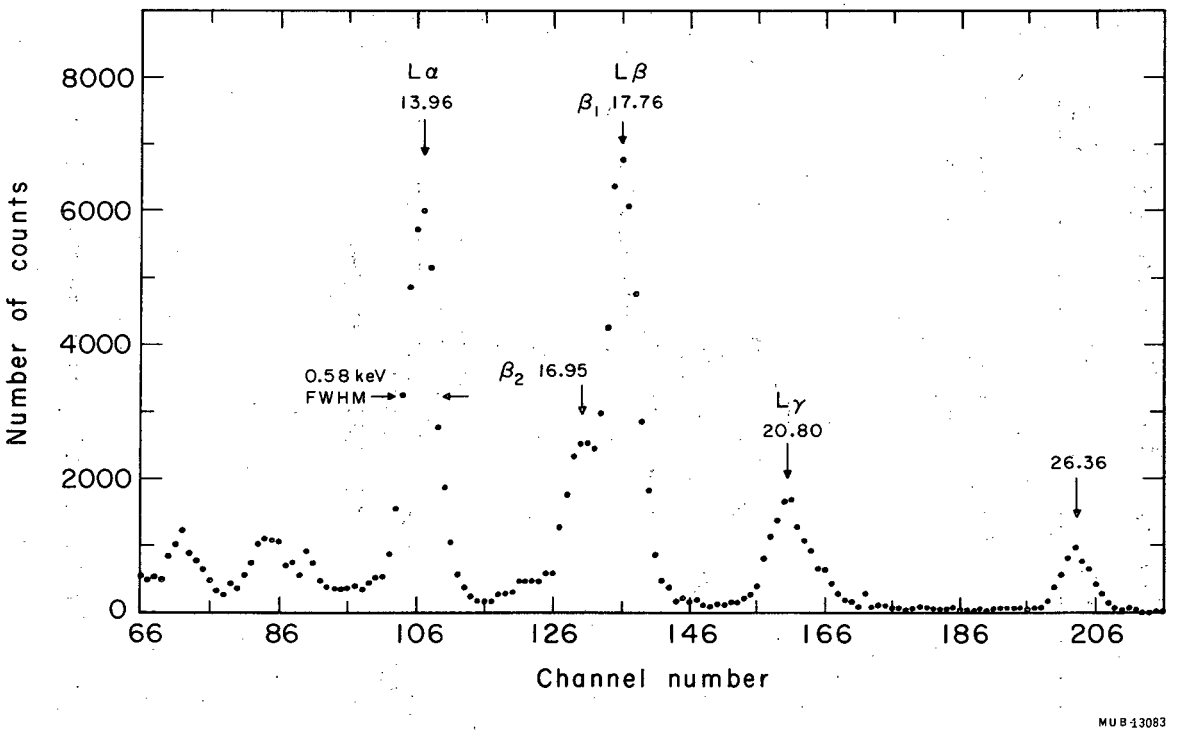

Fig. 14. X-ray spectrum of ^{241}Am.